Progress In Electromagnetics Research C, Vol. 37, 145–157, 2013

DESIGN FILTERS USING TUNABLE E-SHAPED DUAL-MODE RESONATORS FOR LOWER-ULTRA-WIDEBAND AND UPPER-ULTRA-WIDEBAND APPLICATIONS

Yanliang Wu, Cheng Liao*, Xiangzheng Xiong, and Xuanming Zhong

Institute of Electromagnetics, Southwest Jiaotong University, Chengdu 610031, China

Abstract—Two ultra-wideband (UWB) microstrip bandpass filters (BPFs) are proposed by using tunable E-shaped dual-mode microstrip Stepped-Impedance Resonator (SIR). For the lower band filter measurement results show there is a passband of 3.1 GHz to 5.2 GHz and its 3 dB fractional bandwidth is 51%. The UWB upper band filter may be obtained by tuning E-shaped SIR. The measurement results show there is a passband of 6 GHz to 10.6 GHz and its 3 dB fractional bandwidth is 55%. Compared with the similar investigation using the cascade of electromagnetic band gap (EBG)-embedded multiple-mode resonator (MMR) and fork resonator, the proposed approach has some advantages, such as easier adjustment of bandwidths, better passband performances and smaller size etc..

1. INTRODUCTION

In 2002, the US Federal Communications Commission (FCC) approved the use of ultra-wideband (UWB) devices operating in the frequency range of 3.1 to 10.6 GHz [1]. Since then, efforts have been made to realize various kinds of filter configurations for the purpose of wideband and ultra-wideband uses [2–7]. In fact there is an issue of a possible electromagnetic interference over the allocated bandwidth of the UWB system, i.e., some narrow bands for other communication systems may exist in this band, such as wireless local area networks (WLANs) [8–10]. Therefore, the direct sequence ultra-wideband (DSUWB) specification for wireless personal area networks (WPANs) may be further divided into a lower band of 3.1–4.9 GHz and an upper band of 6.2–9.7 GHz [11].

Received 18 November 2012, Accepted 4 February 2013, Scheduled 5 February 2013

* Corresponding author: Cheng Liao (c.liao@swjtu.edu.cn).

Recently, the investigation of tunable resonator structures [12–15], which may realize the flexible design of filter for the UWB lower band and upper band, has attracted increasing attention. In previous work, the EBG structure [16] or fork resonator [17] were used for the design of UWB bandpass filter. Based on these studies Habiba et al. [18] proposed a new approach in which the multiple fork resonators and EBG-embedded structures are cascaded and it may design the UWB dual band individually. Unfortunately this approach has some disadvantages, such as the bandwidth of passbands is not easy to adjust, the characteristics of frequency responses still need to be improved and the cascaded multiple resonators may cause a larger circuit dimension etc..

In this paper, firstly a flexible approach of the UWB dual band filter design based on improved tunable E-shaped dual-mode resonators is proposed. Then the Source-Load cross-coupling structure is employed [19–21] for improving the roll-off characteristics of the passband edges and the stopband rejection level. It can be seen that the several disadvantages as discussed earlier are overcome by the proposed approach. Finally, two prototype filters have been designed and fabricated. Good agreements between the simulated and measured results are obtained.

2. FILTERS DESIGN

2.1. Analysis of Dual-mode E-shaped Resonator

The traditional and improved E-shaped microstrip resonators are illustrated in Figure 1. As shown in Figure 1(a), the traditional E-shaped resonator has a symmetrical structure, and it consists of a

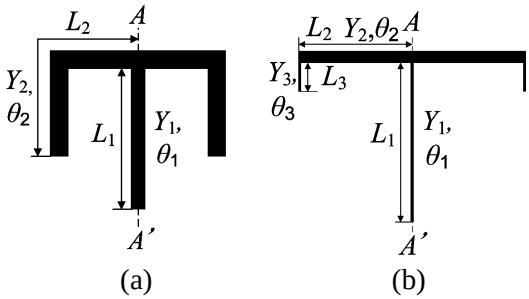

Figure 1. Configuration of E-shaped resonator. (a) Traditional E-shaped resonator. (b) Improved E-shaped resonator.

uniform half-wavelength resonator with the characteristic admittance Y_2 and electric length $2\theta_2$ and an open-circuited stub with the characteristic admittance Y_1 and electric length θ_1 in the centre of the uniform half-wavelength resonator. For obtaining a compact size, uniform half-wavelength resonator is bent and then the traditional E-shaped resonator is formed. Actually, this structure may also be considered as a stub-loaded resonator [22–24]. In previous reports, traditional E-shaped resonator structures are basically used for the design of narrow band (fractional bandwidth less than 10%) filters and seldom be used in the design of wideband filters [25–27].

Figure 1(b) shows the improved tunable E-shaped dual-mode microstrip resonators. In this improved structure, stepped impedance resonator (SIR) [28–31] is used in stead of uniform half-wavelength resonator which can provide additional characteristic admittance Y_3 and electric length θ_3 for tuning resonance frequency more flexible. The open-circuited stub at the centre of the E-shaped SIR introduces another transmission pole near the fundamental resonance frequency of the SIR. Therefore the proposed structure is a dual-mode resonator [32–34].

Figures 2(a) and (b) show the current patterns of the two fundamental eigenmodes. As shown in Figure 2(a), the surface current

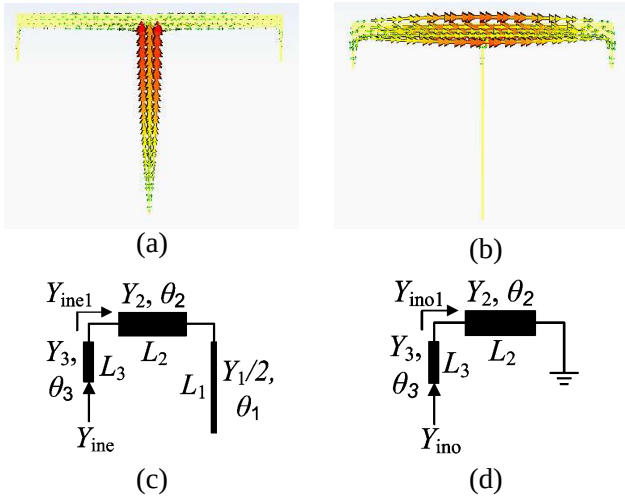

Figure 2. Surface current pattern and equivalent circuit. (a) Surface current pattern at the resonance frequency of even mode. (b) Surface current pattern at the resonance frequency of odd mode. (c) Equivalent circuit of even-mode resonance. (d) Equivalent circuit of odd-mode resonance.

of the middle stub splits up into two parts flowing into the left- and right-branches, which is symmetric with respect to the middle-axes; this mode thus behaves as an even mode. On the other hand, the surface current in Figure 2(b) is dominant only in left- and right-branches, and the mode is an odd mode.

For even-mode excitation, the approximate equivalent circuit is shown in Figure 2(c). The resulting input admittance for even-mode can be expressed as

$$Y_{ine} = Y_3 \cdot \frac{Y_{ine1} + jY_3 \tan\theta_3}{Y_3 + jY_{ine1} \tan\theta_3} \tag{1}$$

where

$$Y_{ine1} = jY_2 \cdot \frac{Y_2 \tan\theta_2 + (Y_1 \tan\theta_1)/2}{Y_2 - (Y_1 \tan\theta_1 \tan\theta_2)/2} \tag{2}$$

where $\theta_1 = \beta L_1$, $\theta_2 = \beta L_2$, $\theta_3 = \beta L_3$ and β is the propagation constant. In this case, the propagation constant is almost equal for even-mode and odd-mode. The resonance condition is

$$Y_{ine1} + jY_3 \tan\theta_3 = 0 \quad (\text{at } f = f_e) \tag{3}$$

f_e is the frequency of even-mode. From Eq. (3), the even-mode resonance frequency can be determined. Figure 2(d) shows the odd-mode equivalent circuit. Similarly, the input admittance for odd-mode can be given by

$$Y_{ino} = jY_3 \cdot \frac{Y_3 \tan\theta_3 - Y_2 \cot\theta_2}{Y_3 + Y_2 \cot\theta_2 \tan\theta_3} = 0 \tag{4}$$

Then, Eq. (4) can be derived as

$$Y_3 \tan\theta_3 = Y_2 \cot\theta_2 \tag{5}$$

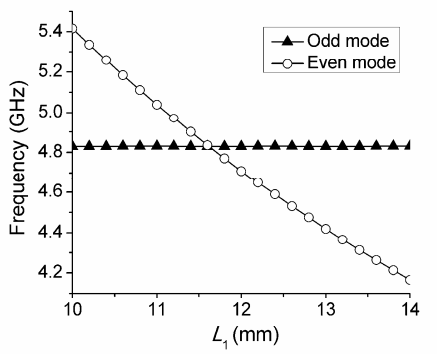

Figure 3. Resonance frequencies of the degenerate modes against the size where $\varepsilon_r = 2.2$; $h = 0.508\,\text{mm}$, $l_2 = 13\,\text{mm}$, and $l_3 = 2.5\,\text{mm}$.

Figure 3 shows the resonance frequencies of the two modes against L_1. The horizontal axis is the length of the middle branch L_1. The vertical axis is the resonator frequency of even mode and odd mode. As is shown in Figure 3, when L_1 varies from 10 mm to 14 mm, the resonance frequency of the even mode decreases almost linearly from 5.4 to 4.2 GHz, meanwhile the resonance frequency of the odd mode is almost constant (around 4.82 GHz).

2.2. UWB Lower Band and Upper Band Filters Design

The configuration of the UWB lower band filter is shown in Figure 4(a), to obtain much tighter coupling between the input/output ports and the E-shaped SIR, the capacitive S-L cross-coupled feed structure is proposed in this filter. The coupling scheme is shown in Figure 4(b) and the signal transmits from port 1 to port 2 through two paths: the signal of path 1 is mainly coupled into the E-shaped resonator through a parallel coupling-line structure; meanwhile, the direct signal of path 2 from port 1 to port 2 through weakly coupling is formed by capacitive S-L cross-coupled feed structure. Beyond the passband, transmission zeros may generate owing to the interaction of the signals from the two coupling paths.

With the coupling scheme shown in Figure 4(b), the corresponding coupling matrix M can be given by [35]

$$\begin{bmatrix} 0 & M_{S1} & M_{S2} & M_{SL} \\ M_{S1} & M_{11} & 0 & M_{1L} \\ M_{S2} & 0 & M_{22} & M_{2L} \\ M_{SL} & M_{1L} & M_{2L} & 0 \end{bmatrix} \tag{6}$$

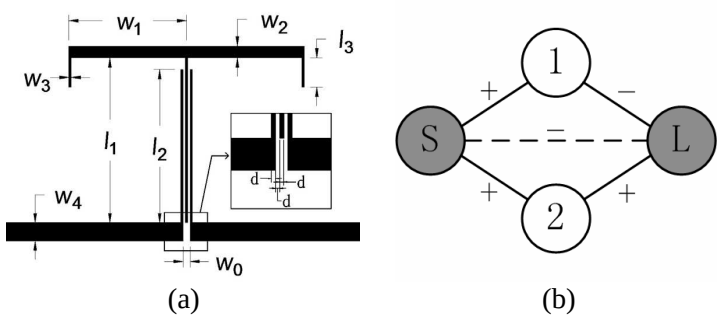

Figure 4. Layout of UWB lower band filter. (a) Proposed lower-UWB BPF. (b) Corresponding coupling scheme (1 and 2 represent the odd and even mode respectively).

The proposed filter has an inherent transmission zero. To get more insight of how to control inherent transmission zero in this configuration, an explicit expression relating the coupling elements and the transmission zero Ω is provided in a low-pass prototype as follows:

$$\Omega = \frac{M_{11}M_{S2}^2 - M_{22}M_{S1}^2}{M_{S1}^2 - M_{S2}^2} \tag{7}$$

The mapping between normalized frequency ω' and actual frequency f is $\omega' = (f/f_0 - f_0 - f_0/f)\Delta f/f_0$, where f_0 and Δf are center frequency and bandwidth of filter, respectively. In a more explicit expression, M_{11} and M_{22} can be related to the odd mode resonant frequency f_{odd} and even mode resonant frequency f_{even}, as follows:

$$f_{odd} = f_0\left(1 - \frac{M_{11} \times \Delta f}{2f_0}\right) \tag{8}$$

$$f_{even} = f_0\left(1 - \frac{M_{22} \times \Delta f}{2f_0}\right) \tag{9}$$

If $M_{11} > 0$ and $M_{22} < 0$, the transmission zero Ω would be greater than zero and $f_{even} > f_0 > f_{odd}$. The inherent transmission zero would be on the upper stopband. On the other hand, if $M_{11} < 0$ and $M_{22} > 0$, the transmission zero Ω would be less than zero and $f_{even} < f_0 < f_{odd}$. The inherent transmission zero would be on the lower stopband. Another mathematic express for the transmission zeros may be incorporated (7) and (9)

$$\Omega \cdot (f_{even} - f_0) = \frac{-M_{22} \times \Delta f}{2} \times \frac{M_{11}M_{S2}^2 - M_{22}M_{S1}^2}{M_{S1}^2 - M_{S2}^2} \tag{10}$$

The right part of Eq. (10) is always positive regardless $M_{22} > 0$ or $M_{22} < 0$. Therefore, as we have seen, the inherent transmission zero is always at the same side of passband with even mode. In this proposed improved dual-mode E-shaped SIR, as shown in Figure 3, when L_1 varies from 10 mm to 14 mm, the resonance frequency of the even mode decreases almost linearly from 5.4 to 4.2 GHz, while the resonance frequency of the odd mode is almost constant (around 4.82 GHz). As a result, we can adjust the position of inherent transmission zero flexibly by tuning the length of L_1.

In additional, the capacitive S-L coupling structure can introduce an additional transmission zero locate in upper-stopband. In practice, the proposed tighter coupling capacitive S-L cross-coupled feed structure which is shown in Figure 5(a) can introduce three transmission zeros which are distributed in lower and upper stopbands.

As shown in Figure 5(b), if fixing $l_1 - l_2 = 1$ mm and tuning the length of l_1, it is clearly observed that the passband move downwards when l_1 increases from 13 mm to 15 mm. Therefore, the operating frequency of the filter can be changed flexibly through varying the length of l_1.

According to the above analysis, the proposed UWB lower band filter was fabricated on the Rogers RT/duroid 5880 substrate board with dielectric constant $\varepsilon_r = 2.2$, loss tangent $\tan\delta = 0.0009$, and thickness of 0.508 mm. The final dimensions of the filter are as follows: $l_1 = 14$ mm, $l_2 = 13$ mm, $w_1 = 10$ mm, $w_2 = 1$ mm, $w_3 = 0.2$ mm. The simulated and measured results of the filter are shown in Figure 6. The measured results show there is a passband of 3.1 GHz to 5.2 GHz, and the 3 dB fractional bandwidth is 51%. The size of the filter is

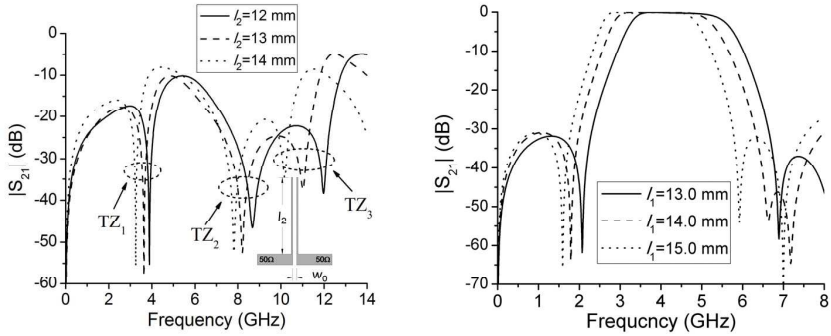

Figure 5. Simulated frequency response. (a) Simulated S_{21} magnitude of the S-L cross-coupled feed structure. (b) Controlling of the operating frequency of UWB lower band filter.

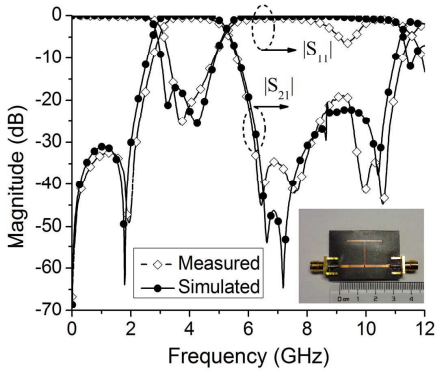

Figure 6. Simulated and measured results and photograph of the proposed UWB lower band filter.

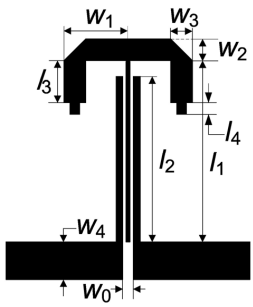

Figure 7. Layout of UWB upper band filter.

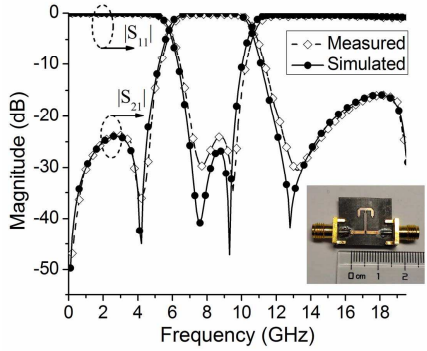

Figure 8. Simulated and measured results and photograph of the proposed UWB upper band filter.

1.5 cm × 2 cm, i.e., $0.28\lambda_g \times 0.38\lambda_g$, where λ_g is the guide wavelength at the centre frequency of the passband.

Furthermore, due to the improved E-shaped dual-mode resonator can provide additional characteristic admittance Y_3 and electric length θ_3 for tuning resonance frequency more flexibly. Therefore compared with traditional E-shaped resonator the resonance frequencies of the presented E-shaped resonator may be tuned more flexibly through adjusting three characteristic admittance and electric length. Based on the identical design approach, the UWB upper band filter has been designed and fabricated. The configuration of the filter is shown in Figure 7.

The final dimensions of the UWB upper band filter are as follows: $w_0 = 0.44$ mm, $w_1 = 2.63$ mm, $w_2 = 0.89$ mm, $l_1 = 7.48$ mm, $l_2 = 6.83$ mm. The filter was also fabricated on the Rogers RT/duroid 5880 substrate board with dielectric constant $\varepsilon_r = 2.2$, that the same as the previous design. The simulated and measured results of the filter are shown in Figure 8. The measured results show the 3 dB passband covers the range of 6 GHz to 10.6 GHz, and it has a fractional bandwidth of 55%. Furthermore, although a low dielectric constant substrate was used, the size of the filter still keeps relatively small which is 0.5 cm × 0.84 cm, i.e., $0.19\lambda_g \times 0.32\lambda_g$.

3. PERFORMANCE COMPARISONS

For visually compared with the previous investigation, the simulated and measured frequency response curves of Ref. [18] are approximately extracted and combine them with the curves of this work, as shown

in Figure 9 and Figure 10 respectively. As shown in Figure 9(a) and Figure 10(a), the results of the UWB lower band and upper band presented in Ref. [18] show some deviations from the actual UWB dual band.

On the other hand, it may be observed in Figure 9(b) and Figure 10(b) that the passband insert loss and return loss of Ref. [18] still need to be improved. The reason is that the structure of the cascading multiple EBG-embedded resonators and fork resonators is difficult to flexibly tune the UWB lower band and upper band. In a word this method may exist some disadvantages, i.e., difficult to adjust the bandwidths individually, relatively large insert and return loss, larger circuit size etc.. In this paper, a single tunable E-shaped dual-model resonator is proposed and it may overcome these drawbacks properly.

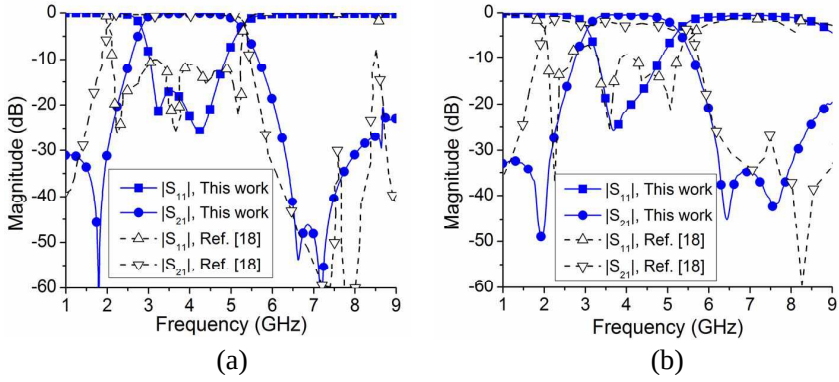

Figure 9. Comparison of frequency response curves of UWB lower band filter. (a) Simulated results. (b) Measured results.

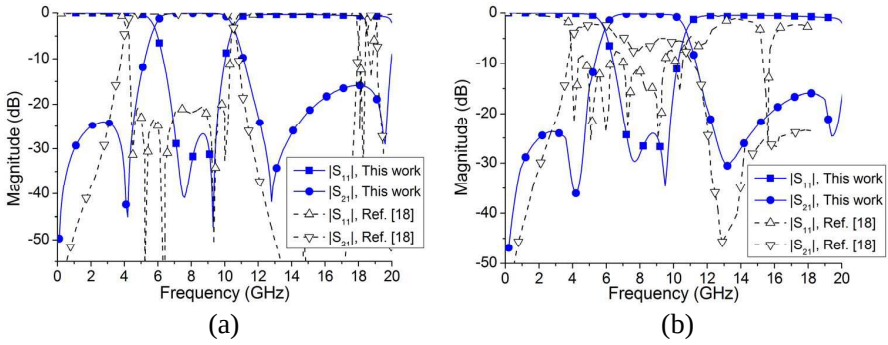

Figure 10. Comparison of frequency response curves of UWB upper band filter. (a) Simulated results. (b) Measured results.

Table 1. compares performance characteristics with the similar study [18].

Reference	3 dB bandwidths (GHz)	Fractional bandwidths	Substrate (ε_r, h (mm))	Size (mm × mm)
Ref. [18]	1.9–5.5 and 5–10	97% and 67%	4.4, 1.6	3×64.3 and 4.8×32.3
This work	3.1–5.2 and 6–10.6	51% and 55%	2.2, 0.508	15×20 and 5×8.4

Table 1 summarizes some more specifics features for comparison.

4. CONCLUSIONS

In this paper, a flexible design approach of the UWB lower band and upper band filter in which the improved tunable E-shaped dual-mode resonators are used is proposed. Two prototype filters have been designed and fabricated. The simulated and measured results show good agreement. Compared with the previous work the proposed method has some advantages such as easier adjustment of bandwidths, better passband performances and smaller size etc..

ACKNOWLEDGMENT

This work was supported by the National Basic Research Program of China (973 Program, Grant No. 2013CB328904), the Open Research Fund of Key Laboratory of Cognitive Radio and Information Processing of Ministry of Education of China (Grant No. 2011KF05), and the Fundamental Funds of the Central Universities.

REFERENCES

1. Federal Communications Commission, "Revision of Part 15 of the commission's rules regarding ultra-wideband transmission systems," Tech. Rep. ET-Docket 98-153, FCC 02-48, FCC, 2002.
2. Gao, M.-J., L.-S. Wu, and J. F. Mao, "Compact notched ultra-wideband bandpass filter with improved out-of-band performance using quasi electromagnetic bandgap structure," *Progress In Electromagnetics Research*, Vol. 125, 137–150, 2012.
3. Kuo, J.-T., C.-Y. Fan, and S.-C. Tang, "Dual-wideband bandpass filters with extended stopband based on coupled-line and coupled

three-line resonators," *Progress In Electromagnetics Research*, Vol. 124, 1–15, 2012.

4. Chen, W.-Y., M.-H. Weng, S.-J. Chang, H. Kuan, and Y.-H. Su, "A new tri-band bandpass filter for GSM, WiMAX and ultra-wideband responses by using asymmetric stepped impedance resonators," *Progress In Electromagnetics Research*, Vol. 124, 365–381, 2012.
5. Xu, J., B. Li, H. Wang, C. Miao, and W. Wu, "Compact UWB bandpass filter with multiple ultra narrow notched bands," *Journal of Electromagnetic Waves and Applications*, Vol. 25, No. 7, 987–998, 2011.
6. Liu, C.-Y., T. Jiang, and Y.-S. Li, "A novel UWB filter with notch-band characteristic using radial-UIR/SIR loaded stub resonators," *Journal of Electromagnetic Waves and Applications*, Vol. 25, No. 2, 233–245, 2011.
7. Yang, G., W. Kang, and H. Wang, "An UWB bandpass filter based on single ring resonator and shorted stubs loaded without coupled feed lines," *Journal of Electromagnetic Waves and Applications*, Vol. 25, No. 16, 2159–2167, 2011.
8. Ma, D.-C., Z.-Y. Xiao, L.-L. Xiang, X.-H. Wu, C.-Y. Huang, and X. Kou, "Compact dual-band bandpass filter using folded SIR with two stubs for WLAN," *Progress In Electromagnetics Research*, Vol. 117, 357–364, 2011.
9. Liao, X.-J., H.-C. Yang, and N. Han, "A switchable bandpass filter using pin diodes on/off characteristics for WLAN application," *Journal of Electromagnetic Waves and Applications*, Vol. 25, No. 10, 1402–1411, 2011.
10. Mashhadi, M. and N. Komjani, "Design of novel dual-band bandpass filter with multi-spurious suppression for WLAN application," *Journal of Electromagnetic Waves and Applications*, Vol. 26, No. 7, 851–862, 2012.
11. IEEE.15 Working Group for Wireless Personal Area Networks, "Detailed DS-UWB simulation results," Tech. Rep., IEEE 802.15, 802, 2004.
12. Wang, X.-G., Y.-H. Cho, and S.-W. Yun, "A tunable combline bandpass filter loaded with series resonator," *IEEE Trans. Microw. Theory Tech.*, Vol. 60, No. 6, 1569–1576, 2012.
13. Huang, S.-Y. and Y.-H. Lee, "A compact E-shaped patterned ground structure and its applications to tunable bandstop resonator," *IEEE Trans. Microw. Theory Tech.*, Vol. 57, No. 3, 657–666, Mar. 2009.

14. Wang, X.-H., B.-Z. Wang, H.-L. Zhang, and K.-J. Chen, "A tunable bandstop resonator based on a compact slotted ground structure," *IEEE Trans. Microw. Theory Tech.*, Vol. 55, No. 9, 1912–1917, Sep. 2007.
15. Chen, J.-X., J. Shi, Z.-H. Bao, and Q. Xue, "Tunable and switchable bandpass filters using slot-line resonators," *Progress In Electromagnetics Research*, Vol. 111, 25–41, 2011.
16. Wong, S. W. and L. Zhu, "EBG-embedded multiple-mode resonator for UWB bandpass filter with improved upper-stopband performance," *IEEE Microwave Wireless Comp. Lett.*, Vol. 17, No. 6, 421–423, 2007.
17. Chen, H. and Y.-X. Zhang, "A novel and compact UWB bandpass filter using microstrip fork-form resonators," *Progress In Electromagnetics Research*, Vol. 77, 273–280, 2007.
18. Habiba, H. U., K. Malathi, M. H. Masood, and R. Kunnath, "Tunable electromagnetic band gap-embedded multimode resonators for ultra-wideband dual band, lower-ultra-wideband and upper-ultra-wideband applications," *IET Microw. Antennas Propag.*, Vol. 5, No. 10, 1182–1187, Jul. 2011.
19. Shaman, H. and J.-S. Hong, "A novel ultra-wideband (UWB) bandpass filter (BPF) with pairs of transmission zeroes," *IEEE Microwave Wireless Comp. Lett.*, Vol. 17, No. 2, 121–123, 2007.
20. Liao, C.-K. and C.-Y. Chang, "Design of microstrip quadruplet filters with source-load coupling," *IEEE Trans. Microw. Theory Tech.*, Vol. 53, No. 7, 2302–2308, Jul. 2005.
21. Ho, M.-H. and P.-F. Chen, "Suspended substrate stripline bandpass filters with source-load coupling structure using lumped and full-wave mixed approach," *Progress In Electromagnetics Research*, Vol. 122, 519–535, 2012.
22. Mondal, P. and M. K. Mandal, "Design of dual-band bandpass filters using stub-loaded open-loop resonators," *IEEE Trans. Microw. Theory Tech.*, Vol. 56, No. 1, 150–155, Jan. 2008.
23. Wu, Y. and Y. Liu, "A coupled-line band-stop filter with three section transmission-line stubs and wide upper pass-band performance," *Progress In Electromagnetics Research*, Vol. 119, 407–421, 2011.
24. Huang, X.-G., Q.-Y. Feng, and Q.-Y. Xiang, "High selectivity broadband bandpass filter using stub-loaded quadruple-mode resonator," *Journal of Electromagnetic Waves and Applications*, Vol. 26, No. 1, 34–43, 2012.
25. Liao, C.-K., P.-L. Chi, and C.-Y. Chang, "Microstrip realization

of generalized Chebyshev filters with box-like coupling schemes," *IEEE Trans. Microw. Theory Tech.*, Vol. 55, No. 1, 147–153, Jan. 2007.

26. Kuo, Y.-T. and C.-Y. Chang, "Analytical design of two-mode dual-band filters using E-shaped resonators," *IEEE Trans. Microw. Theory Tech.*, Vol. 60, No. 2, 250–260, Feb. 2012.
27. Wei, C.-L., B.-F. Jia, Z.-J. Zhu, and M.-C. Tang, "Design of different selectivity dual-mode filters with E-shaped resonator," *Progress In Electromagnetics Research*, Vol. 116, 517–532, 2011.
28. Makimoto, M. and S. Yamashita, *Microwave Resonators and Filters for Wireless Communications-theory and Design,* Springer-Verlag, Berlin, Germany, 2001.
29. Liu, S.-K. and F.-Z. Zheng, "A new compact tri-band bandpass filter using step impedance resonators with open stubs," *Journal of Electromagnetic Waves and Applications*, Vol. 26, No. 1, 130–139, 2012.
30. Chen, W.-Y., M.-H. Weng, and S.-J. Chang, "A new tri-band bandpass filter based on stub-loaded step-impedance resonator," *IEEE Microwave Wireless Comp. Lett.*, Vol. 22, No. 4, 179–181, Apr. 2012.
31. Wu, H.-W., Y.-F. Chen, and Y.-W. Chen, "Multi-layered dual-band bandpass filter using stub-loaded stepped-impedance and uniform-impedance resonators," *IEEE Microwave Wireless Comp. Lett.*, Vol. 22, No. 3, 114–116, Mar. 2012.
32. Chen, C.-H., C.-S. Shih, T.-S. Horng, and S.-M. Wu, "Very miniature dual-band and dual-mode bandpass filter designs on an integrated passive device chip," *Progress In Electromagnetics Research*, Vol. 119, 461–476, 2011.
33. Zhang, Z.-G., Y. Fan, Y.-J. Cheng, and Y.-H. Zhang, "A compact multilayer dual-mode substrate integrated circular cavity (SICC) filter for X-band application," *Progress In Electromagnetics Research*, Vol. 122, 453–465, 2012.
34. Zhang, Z.-G., Y. Fan, Y.-J. Cheng, and Y.-H. Zhang, "A novel multilayer dual-mode substrate integrated waveguide complementary filter with circular and elliptic cavities (SICC and SIEC)," *Progress In Electromagnetics Research*, Vol. 127, 173–188, 2012.
35. Thomas, J. B, "Cross-coupling in coaxial cavity filters — A tutorial overview," *IEEE Trans. Microw. Theory Tech.*, Vol. 51, No. 4, 1368–1376, Apr. 2003.